FILTRATION AND DIPERSION OF CARBON NANOTUBES DURING RESIN FILM INFUSION

Baril-Gosselin, S.[1,2], Robitaille, F.[1]*
[1] Department of Mechanical Engineering, University of Ottawa,
Ottawa, Canada
[2] Automotive and Surface Transportation, National Research Council Canada,
Boucherville, Canada
* Corresponding author (Simon.Baril-Gosselin@nrc-cnrc.gc.ca)

Keywords: *resin film infusion, carbon nanotubes, fabrics*

ABSTRACT

In this work, resin film infusion (RFI) was used for understanding how processing parameters affect the filtration and dispersion of carbon nanotubes (CNTs) during the manufacturing of epoxy polymer matrix composites (PMCs). This was achieved by investigating two different stacking sequences and different types of fabrics. Results showed that filtration increases with resin flow lengths and that filtration depends significantly on the type of fabric selected. More importantly, CNT filtration correlates well with the resin flow permeability of fabrics. However, the greatest limitation to a uniform CNT distribution was the agglomeration of CNTs into clusters during processing. In-situ monitoring of resin flow enabled the direct observation and characterisation of CNT agglomeration. Agglomeration was linked to the reduction in resin viscosity during RFI. Processing at lower temperatures was investigated for limiting clustering. This led to a significant reduction in CNT clustering but resulted in increased levels of porosity.

1 INTRODUCTION

Polymer-matrix composites (PMCs) reinforced with 2D woven fabrics have great in-plane specific strength. However, their laminated structure leads to relatively weak interlaminar properties, governed mainly by the matrix. This can be mitigated by improving matrix toughness through the addition of toughening agents. In the last decade, significant effort was made towards producing multi-scale PMCs by modifying the matrix with carbon nanotubes (CNTs) that feature exceptional mechanical properties, e.g. elastic modulus and tensile strength were measured at 450 GPa and 3.6 GPa respectively [1].

In reality, the addition of CNTs to the matrix results in modest improvements of the interlaminar shear strength of PMCs, approximately 10% to 15% for a 0.3 wt% CNT loading [2–4]. Limited improvements to the interlaminar shear strength are caused in part by heterogeneous matrix properties resulting from CNT clustering and CNT filtration.

CNT clustering occurs due to the great aspect ratio of CNTs and strong van der Waals forces between CNTs. The agglomeration of CNTs results in matrix regions of high CNT content which are highly reinforced, and regions of low CNT content which are weaker. There are different methods available to exfoliate CNTs and disperse them in a matrix, including the use of great shear stresses, ultra-sonication and use of surfactants [5–7]. More importantly, better dispersion of CNTs can be achieved by improving the compatibility between the resin matrix and CNTs through the functionalisation of CNTs [6, 8, 9].

CNT filtration can be a major source of matrix heterogeneity in multi-scale PMCs processed through infusion methods (Figure 1). This is because the dense fibre network of fabrics is quite effective at filtering CNT clusters. Studies [8, 10] have showed that filtering can be lessened by improving the dispersion of CNTs. However, there are no exhaustive studies regarding the effect that the fabric architecture has on the filtration of CNTs.

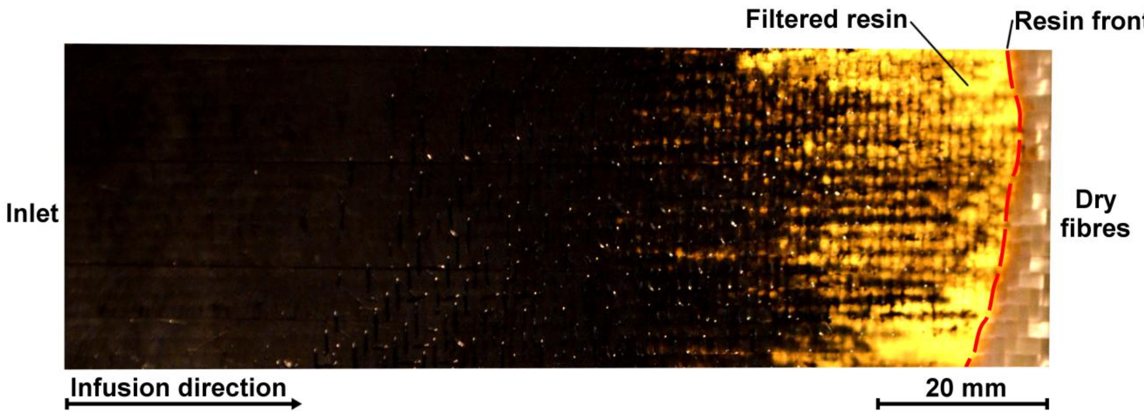

Figure 1: CNT filtration after in-plane resin infusion

The main objective of this work was to investigate the effects that the film stacking sequence and fabric architecture have on the filtration and dispersion of CNTs during resin film infusion (RFI). In RFI, hot-melt resin films are laid between fabric layers with various levels of interleaving, which results in through-thickness resin flow. In this work, two stacking sequences were investigated: bulk RFI which features no interleaving, and interleaved RFI which features complete interleaving of resin films and fabric layers. The work also compared 6 different fabrics that feature different constructions and surface densities. The investigation of these parameters enabled complete characterisation of through-thickness filtration of CNTs in RFI. In addition, in-situ monitoring of RFI provided direct observation of the CNT clustering process, which enabled the proposal of a method for reducing CNT clustering.

2 METHODOLOGY

2.1 Materials

Hot-melt nano-modified epoxy LEO 2397 from Nanoledge (now Axson) was used for investigating filtration and dispersion of CNTs during RFI processing. The resin was supplied in film form and was reinforced with 0.3 wt% of functionalised CNTs (Baytubes® C 150 P). Resin viscosity appears in Figure 3. Transmitted light microscopy (Figure 2) shows that CNTs are originally grouped in very small clusters that are well dispersed in the epoxy.

Filtration of CNTs during RFI was investigated with 5 different carbon fibre fabrics and 1 glass fibre fabric. The construction, surface density, cover factor and transverse permeability of the fabrics appear in Table 1.

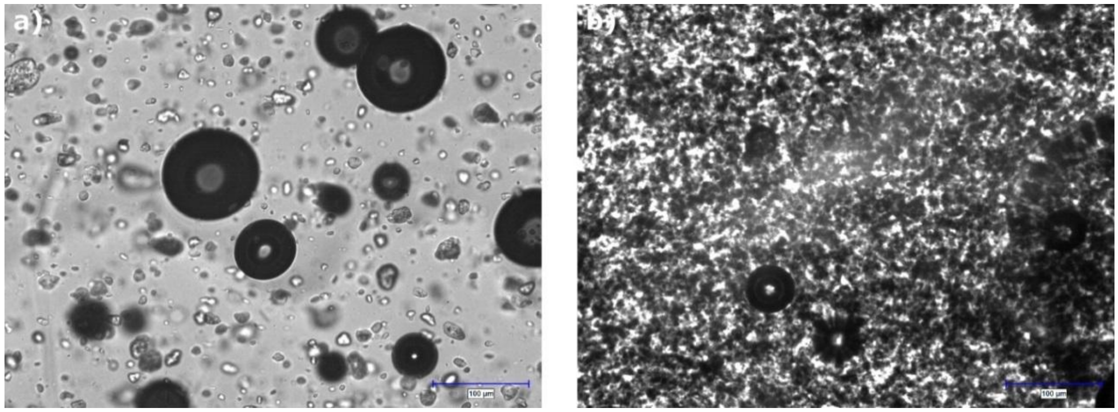

Figure 2: Transmitted light microscopy of a) neat epoxy resin film and b) nano-modified epoxy resin film featuring 0.3 wt% CNTs.

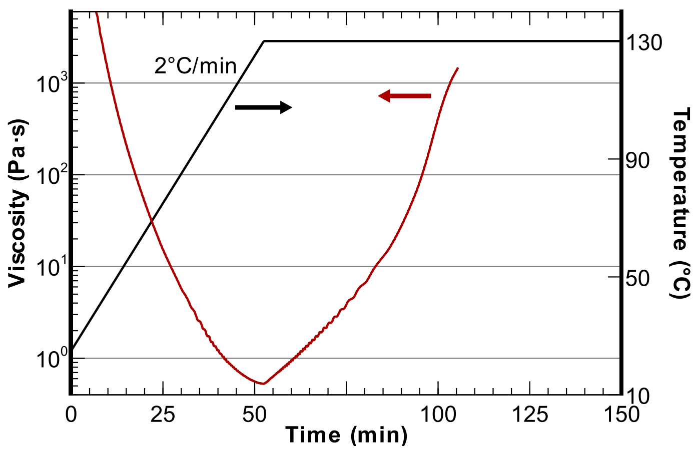

Figure 3: Viscosity profile of epoxy resin LEO 2397 featuring 0.3 wt% CNTs

Table 1: Surface density and transverse permeability values of fabrics

Fabric[a]	Fibres	Construction	Surface density (g/m^2)	Cover factor	Transverse permeability, $V_f = 55\%$ ($10^{-13}\ m^2$)
PW-L	Carbon, HTS40	Plain weave	197	0.928	24.3 ± 1.4
Twill-L	Carbon, HTS40	Twill 2×2	215	0.982	5.3 ± 0.2
Twill-H	Carbon, HTS40	Twill 2×2	429	0.998	26.8 ± 1.6
NCF-L	Carbon, HTS40	NCF, tricot	250	0.996	2.6 ± 0.2
NCF-H	Carbon, HTS40	NCF, chain stitched	534	0.992	10.8 ± 1.0
Twill-G	E-glass	Twill 2×2	315	-	17.3 ± 1.2

Note: [a] suffixes *L* and *H* denotes low and high surface density fabrics featuring carbon fibres, and suffix *G* denotes a glass fibre fabric

2.2 *Manufacturing*

Two RFI stacking sequences were investigated for producing multi-scale PMCs: bulk RFI and interleaved RFI (Figure 4). In bulk RFI, separate stacks of fabric reinforcements and resin films are prepared and superimposed. This results in resin flowing across the entire thickness of a fabric stack during processing. In interleaved RFI, a single stack is made from layering fabric reinforcement plies and resin films alternatively. This results in very short resin flow lengths. The number of fabric plies and resin films in bulk RFI and interleaved RFI stacks were selected for obtaining 4 mm thick PMCs with the carbon fibre fabrics. Additionally, a 10 mm thick PMC made with the bulk RFI stacking sequence was produced with glass fibre fabric Twill-G.

Multi-scale PMCs were manufactured using out-of-autoclave RFI. Stacks of fabric layers and resin films were laid between a glass tool and aluminium caul plate. Consolidation was performed under a vacuum bag. Heat was provided by a flexible electric heater (HR5466, MINCO) bonded to the aluminium caul plate and was controlled using a hysteresis controller with a ±1°C threshold. Cure cycle for the PMCs appears in Figure 3.

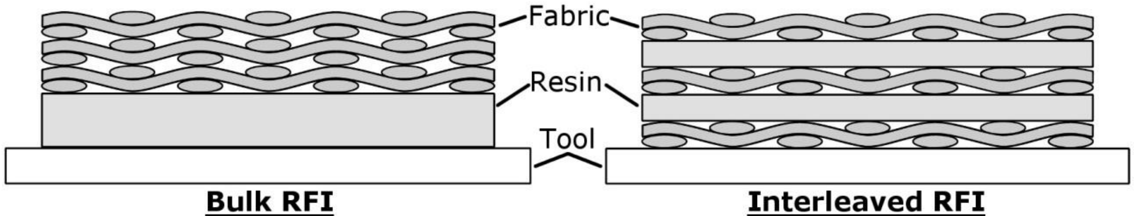

Figure 4: Bulk RFI (top) and interleaved (bottom) stacking sequence

2.3 *Dispersion and filtration of CNTs*

Dispersion and filtration of CNTs was investigated by comparing resin regions that featured low and high CNT contents. Regions of low CNT contents were transparent to light while regions of high CNT contents were pitch black. The distribution of CNTs was obtained by taking the ratio of black regions to the total area of analysis. Measurements were achieved through contrast analysis using software ImageJ (Version 1.49). The distribution of CNTs was investigated on the out-of-plane surfaces of PMCs, and on thin PMC cross-sections through transmitted light microscopy.

3 RESULTS

3.1.1 Bulk RFI

A 10 mm thick multi-scale PMC was fabricated successfully using the bulk RFI stacking sequence with fabric Twill-G. Visual inspection of the PMC showed that inter-yarn regions were black on both the resin and fabric sides, suggesting that some CNTs flowed across the entire laminate during RFI (Figure 5). Inspection of the thin cross-section of the PMC showed that the resin films lost their relatively uniform distribution of CNTs during processing (Figure 6). Hence, compatibility between CNTs and the resin was not sufficiently good to prevent re-agglomeration of CNTs into clusters. Analysis of the cross-section revealed that filtration of CNTs occurred mostly in the first fabric layers of the fabric stack (Figure 7). This suggests that larger CNT clusters are filtered quickly while smaller clusters can flow between yarns without much restriction. In addition, very few regions rich in CNTs were observed in yarns due to significant filtering by the dense fibre network.

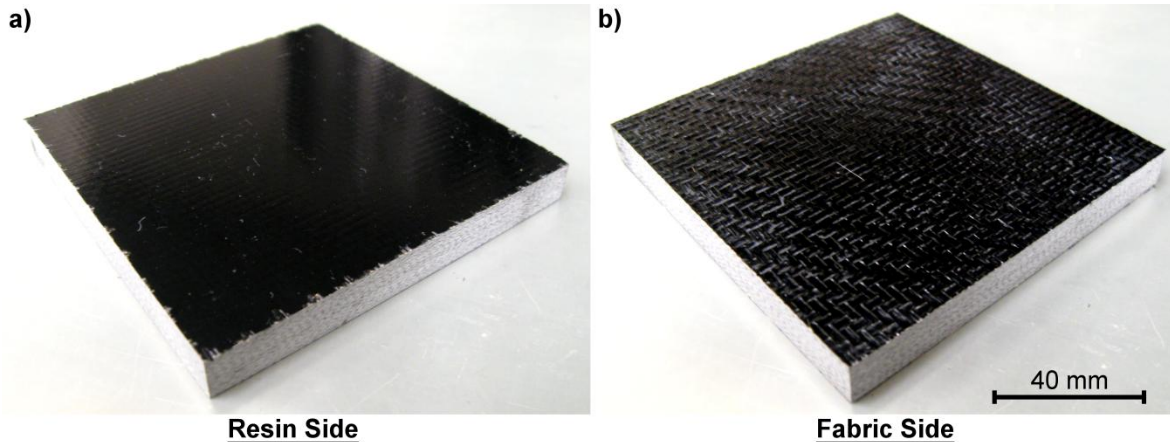

Figure 5: PMC featuring fabric Twill-G after through-thickness infusion using the bulk stacking sequence, a) resin side and b) fabric side

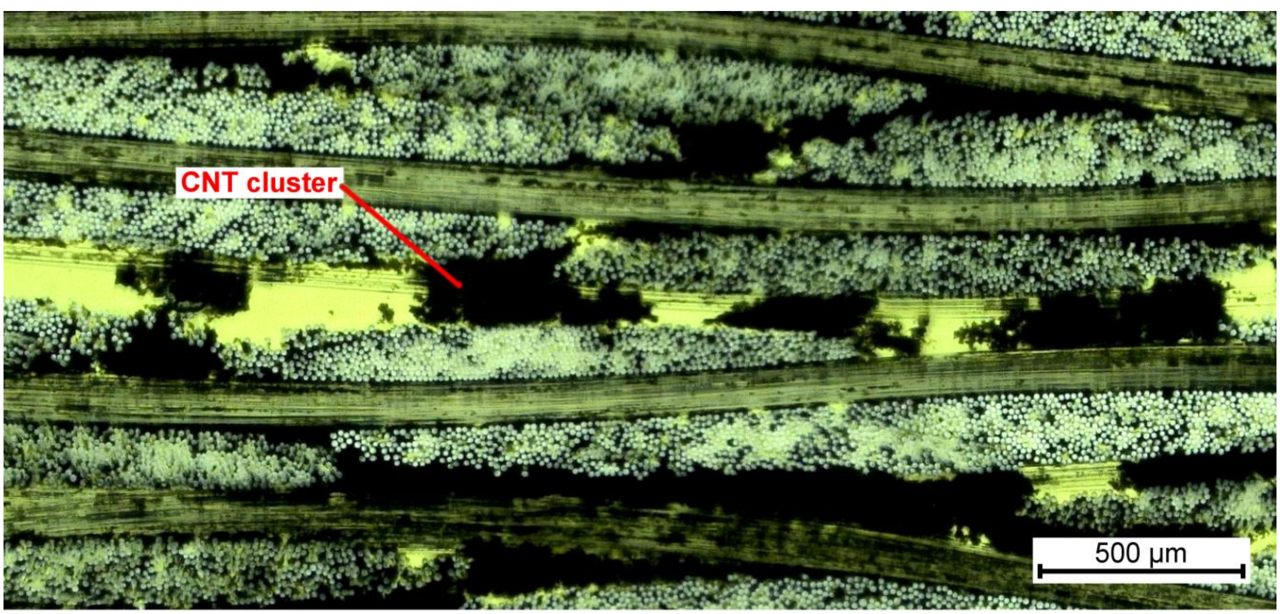

Figure 6: Cross-section of PMC featuring fabric Twill-G observed through transmitted light microscopy showing the distribution of CNTs

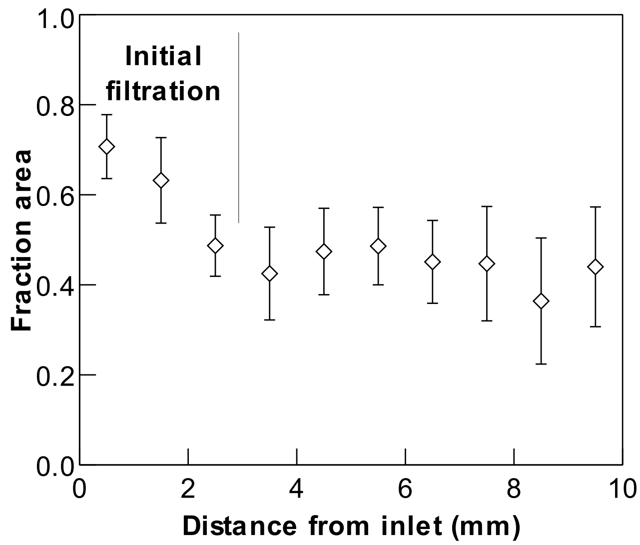

Figure 7: Fraction area of CNT rich regions across the thickness of PMC with fabric Twill-G

The effect that the fabric architecture has on CNT filtration during through-thickness flow was studied with carbon fibre PMCs. Visual inspection of the resin and fabric sides of the PMCs showed that inter-yarn regions were populated with CNT clusters, and that the fabric side of PMCs featured fewer clusters, indicating filtration (Figure 8).

Quantitative analysis of CNT filtration was achieved by comparing the fraction area of the top (fabric) and bottom (resin) sides of PMCs that are covered in CNTs. Results appearing in Figure 9 show significant influence of the fabrics on CNT filtration. For example, no filtration was observed for the PMC featuring fabric Twill-H, while complete filtration occurred with fabric NCF-L. Results showed that for both twills and NCFs, filtration decreased with increasing fabric surface density. Twill fabrics also led to less filtration than NCF fabrics. Finally, comparing fabrics PW-L and Twill-L, it can be seen that the reduction in fabric cover factor reduced filtration markedly. These differences in filtration between fabrics are all explained by the number and size of inter-yarn gaps. Moreover, results showed that the transverse permeability of the fabrics is a good indicator for filtration as the trends for CNT filtration (Figure 9) correlate well with the trends for the transverse permeability of fabrics (Table 1).

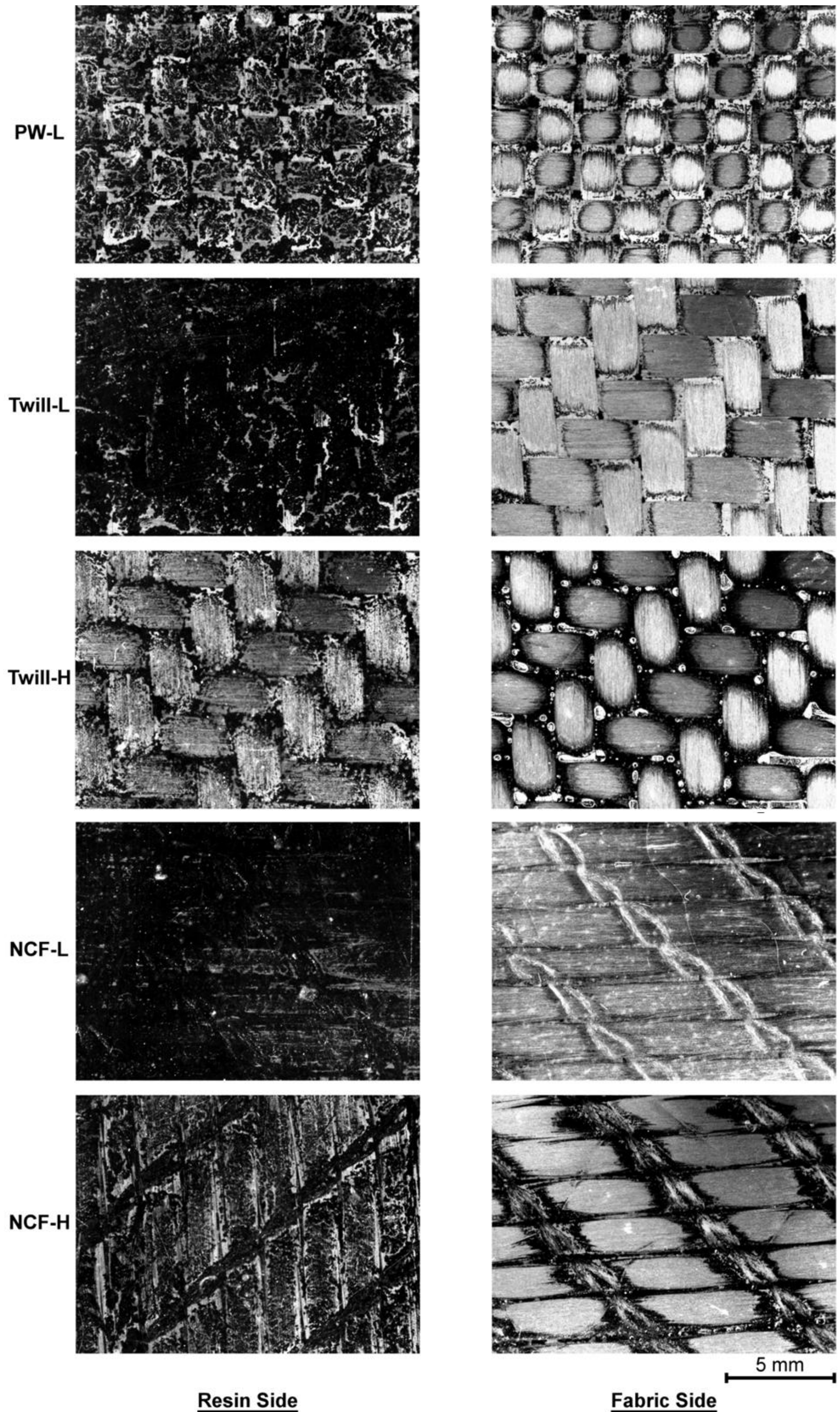

Figure 8: CNT distribution on the resin and fabric sides of bulk RFI PMCs

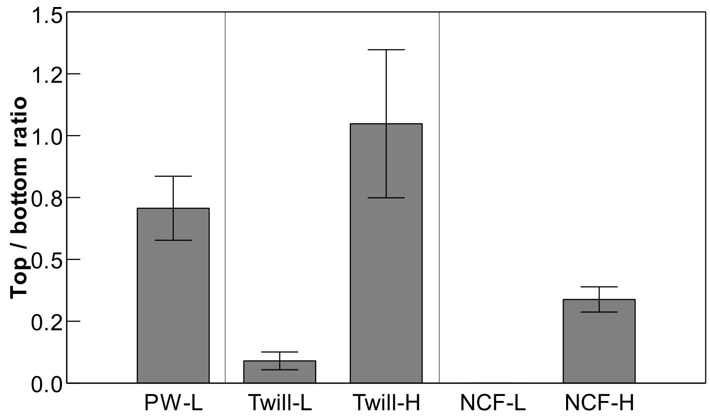

Figure 9: Ratio of the fraction area of the top (fabric) to bottom (resin) sides of the PMCs that are covered in CNTs for bulk RFI

3.1.2 Interleaved RFI

The effect of CNT filtration between fabric plies was eliminated by using interleaved RFI. This method provided uniform distribution of CNT clusters across all inter-yarn gaps of PMCs, resulting in more homogeneous material properties than bulk RFI. However, interleaved RFI did not prevent CNT clustering or low CNT content in yarns due to filtration.

In-situ observations of RFI processing showed that CNTs were initially well dispersed in the resin but that CNTs began to agglomerate at a temperature of approximately 80°C (Figure 10). This occurred because CNTs mobility increased due to the reduction in resin viscosity. From the viscosity profile of the resin (Figure 3), it follows that the critical viscosity value for this combination of resin and CNTs is approximately 10 Pa·s.

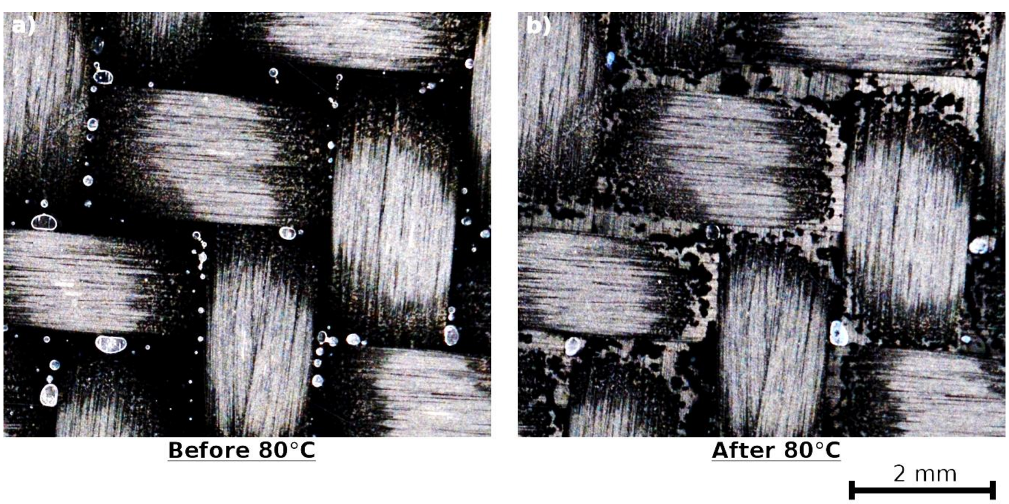

Figure 10: Comparison of the CNT distribution at the surface of a PMC with Twill-L fabric, a) before reaching 80°C, b) after reaching 80°C

4 DISCUSSION AND CONCLUSION

Bulk and interleaved RFI were investigated for manufacturing multi-scale PMCs. Results showed that in the case of bulk RFI, filtration of CNTs during through-thickness resin flow was highly dependent on the architecture of the fabric reinforcements. Interleaved RFI was a viable alternative to reduce filtering of CNTs between fabric layers due to the shorter distances travelled by the resin during infusion. However, CNT distribution in PMCs made with interleaved RFI was not homogeneous because of CNT clustering and CNT filtration by yarns. The greatest obstacle to a uniform distribution of CNTs was the low resin viscosities that are reached during processing. A potential solution consists of manufacturing PMCs at lower temperatures. This was investigated by manufacturing a PMC at 60°C. This resulted in a significant improvement of CNT dispersion (Figure 11). However, it also resulted in a PMC that featured greater levels of porosity; 0.1% porosity for the standard cure at 130°C and 1.2% porosity for a cure at 60°C. Hence, it follows that a good dispersion of CNTs and low porosity content in multi-scale PMCs will only be achieved by improving the compatibility between the CNTs and resin.

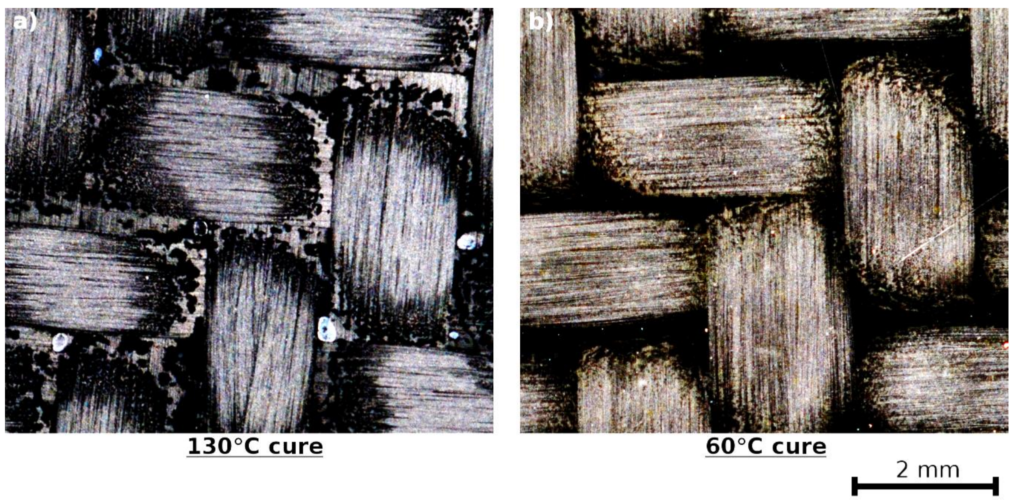

Figure 11: Distribution of CNTs at the surface of a laminate featuring Twill-L textile and L7 resin after a a) standard cure at 130°C and b) low temperature cure at 60°C

5 REFERENCES

[1] Xie S., Li W., Pan Z., Chang B., and Lianfeng S., 2000, "Mechanical and physical properties on carbon nanotube," J. Phys. Chem. Solids, **61**(7), pp. 1153–1158.

[2] Gojny F. H., Wichmann M. H. G., Fiedler B., Bauhofer W., and Schulte K., 2005, "Influence of nano-modification on the mechanical and electrical properties of conventional fibre-reinforced composites," Compos. Part A Appl. Sci. Manuf., **36**(11), pp. 1525–1535.

[3] Sánchez M., Campo M., Jiménez-Suárez A., and Ureña A., 2013, "Effect of the carbon nanotube functionalization on flexural properties of multiscale carbon fiber/epoxy composites manufactured by VARIM," Compos. Part B Eng., **45**(1), pp. 1613–1619.

[4] Wichmann M. H. G., Sumfleth J., Gojny F. H., Quaresimin M., Fiedler B., and Schulte K., 2006, "Glass-fibre-

reinforced composites with enhanced mechanical and electrical properties - Benefits and limitations of a nanoparticle modified matrix," Eng. Fract. Mech., **73**(16), pp. 2346–2359.
[5] Fan Z., and Advani S. G., 2005, "Characterization of orientation state of carbon nanotubes in shear flow," Mech. Eng., **46**, pp. 5232–5240.
[6] Ma P. C., Mo S. Y., Tang B. Z., and Kim J. K., 2010, "Dispersion, interfacial interaction and re-agglomeration of functionalized carbon nanotubes in epoxy composites," Carbon N. Y., **48**(6), pp. 1824–1834.
[7] Liao Y. H., Marietta-Tondin O., Liang Z., Zhang C., and Wang B., 2004, "Investigation of the dispersion process of SWNTs/SC-15 epoxy resin nanocomposites," Mater. Sci. Eng. A, **385**(1–2), pp. 175–181.
[8] Fan Z., Hsiao K., and Advani S. G., 2004, "Experimental investigation of dispersion during flow of multi-walled carbon nanotube / polymer suspension in fibrous porous media," Carbon N. Y., **42**, pp. 871–876.
[9] Shaffer M. S. P., Fan X., and Windle a. H., 1998, "Dispersion and packing of carbon nanotubes," Carbon N. Y., **36**(11), pp. 1603–1612.
[10] Fan Z., Santare M. H., and Advani S. G., 2008, "Interlaminar shear strength of glass fiber reinforced epoxy composites enhanced with multi-walled carbon nanotubes," Compos. Part A Appl. Sci. Manuf., **39**(3), pp. 540–554.